Journal of Ultrafine Grained and Nanostructured Materials
https://jufgnsm.ut.ac.ir
Vol. 57, No.1, June 2024, pp. 92-103
Print ISSN: 2423-6845 Online ISSN: 2423-6837
DOI: 10.22059/jufgnsm.2024.01.11

Conductive nanofibrous scaffold based on polyvinyl alcohol/ cellulose nanocrystals/ reduced graphene oxide composite reinforced with curcumin for wound healing

Bakhshali Massoumi[1], Raana Sarvari[2,3,4,*], Elaheh Fakhri[5], Khadijeh Emami Rad[1]

[1]Department of Chemistry, Payame noor University, Tehran, Iran;
[2]Infectious and Tropical Diseases Research Center, Tabriz University of Medical Sciences, Tabriz, Iran;
[3]Sarvaran Chemie Pishro Company(S.C.P), Tabriz, Iran;
[4]Stem Cell Research Center, Tabriz University of Medical Sciences, Tabriz, Iran;
[5]Dental and Periodontal Research Center, Faculty of Dentistry, Tabriz University of Medical Sciences, Tabriz, Iran.

Recieved: 18 November 2023; Accepted: 15 June 2024
**Corresponding author email: raanasarvari@yahoo.com*

ABSTRACT

Conductive polymers offer great potential in skin tissue regeneration due to the promoted cellular activity and accelerate healing process. Herein, a polymeric nanofibrous dressing was prepared based on oxidized-nanocrystal cellulose/aminated reduced graphene oxide and polyvinyl alcohol (AD-CNCs/NH_2rGO/PVA) to enhance cell proliferation with electrical fields for wound healing. For this purpose, CNCs were produced from cotton cellulose and oxidized in the presence of sodium periodate. Following the synthesis of rGO and its functionalization with amine, the cross-link between oxidized CNCs and NH_2rGO was created by the Schiff-base reaction. The prepared nanocomposite was mixed with PVA and different proportions of curcumin. The polymeric nanofibrous scaffolds were prepared by electrospinning. With the increase in curcumin content, the hydrophobicity of the composition and the diameter of the nanofibers increased, while the uniformity and mechanical properties were optimized. The PVA/AD-CNCs/NH_2rGO/curcumin nanofibrous scaffold exhibited electrical conductivity and satisfactory thermal stability. The PVA/AD-CNCs/NH_2rGO/curcumin biodegradable nanofibrous scaffold was biocompatible and presented a satisfactory performance in cell attachment, proliferation and spreading, requirements for wound healing purposes.

keywords: *Conductive nanofibrous; PVA; Cellulose nanocrystals; Wound healing; rGO.*

1. Introduction

The wound healing process is a complex but coordinated cascade of cellular interactions starting automatically after injury leading to save skin integrity [1]. This natural, time-consuming process has a severe impact on patient's health due to the possibility of inflammation, bacterial infection, even amputation and reducing the quality of life [2]. In addition, sometimes with special conditions such as infected or chronic wounds including diabetic ulcers, the biological event of healing seems to be ineffective for wound closure, therefore application of supplementary equipment is required [1]. Various poultices and compounds have been evaluated as a salve for the optimal treatment of wounds to promote the healing process and prevent scar tissue formation [3, 4]. Further developments have yielded biomaterials, composed of both synthetic and natural polymers, efficient in wound healing and hemorrhage control while exhibiting other crucial properties including non-toxicity, inertness, non-antigenicity, bio-adhesion, bio-compatibility, antimicrobial properties and bio-degradability [5]. However, traditional wound dressings only passively cover the injury site and their therapeutic effect is highly reliant on the biomolecules released from them [6, 7].

Unimpaired healthy skin exhibits a transepithe-

lial potential (TEP) of up to 100 mV across the epidermis, varying based on the anatomical part [8]. Injury to the skin disrupts the TEP, generating an endogenous electrical field (EF) channeled from the normal skin to the site of injury. This phenomenon guides cell orientation, migration and proliferation, promotes tissue growth, and regulates angiogenesis and re-epithelialization [9]. The electroactive dressings engineered from conductive polymers create a channel transmitting endogenous bioelectric signals to the wound in order to promote the proliferation and differentiation of electrical stimuli-responsive cells and consequently accelerate the wound healing process. Inspired by the endogenous EF of the injury site, several current studies have shown that conductive materials not only can regulate cellular activities in acute wounds but also can be beneficial in treating chronic diseases such as diabetic ulcers [10, 11]. Pathogenesis of chronic or non-healing ulcers is mainly associated with the prolonged presence of myeloid cells due to increased expression of pro-inflammatory cytokines and imbalanced oxidative stress leading to necrotic tissues [1]. It seems that applying electroactive material containing conductivity comparable to the natural skin, on the wound bed to stimulate the endogenous current can correct the imbalance and modulate the behavior of macrophages, neutrophils and keratinocytes as a beneficial way to accelerate wound healing [12, 13].

Among various known conductive polymers, studies mostly used polyaniline, polypyrrole and polythiophene, however, their inherent limitations such as poor mechanical properties necessitate chemical modification or physical blending with non-conductive polymers [14-17]. Notwithstanding, important limitations exist with regard to these conductive materials including toxicity, non-degradability, and difficult performance [8].

Owing to its biocompatibility, biodegradability, hydrophilicity, water-holding capacity and various biological activities, cellulose has been employed for the development of wound dressings and skin substrates. Cellulose-based scaffolds have been recommended as temporary dressings for the treatment of wounds, including critical wounds, second-degree burns, skin graft sites, post-traumatic abrasions and tears, and tissue removal sites by surgeons [6, 18, 19]. A crucial feature of a favorable skin repair material is the ability to absorb wound secretions during the dressing process and remove it from the wound surface after healing which is one of the limitations of traditional wound dressings. The hydrophilic nature of cellulose contributes to creating a moist environment for an improved healing process and acts as a barrier to microorganisms and prevents post-operative adhesion [20].

In order to meet the structural characteristics of a scaffold, a synthetic polymer must be incorporated into the cellulose-based formulation [21]. Polyvinyl alcohol linear polymer is widely used in the field of wound dressing production due to low protein absorption, water solubility, chemical resistance, hydrophilicity, non-toxicity, biodegradability, non-carcinogenicity, swelling ability and biocompatibility [22]. However, cellulose and PVA are naturally lacking conductivity properties. Therefore, in this study, we intend to combine the conductivity of the carbonous materials with the biological properties of cellulose/PVA-based scaffold to develop an electrical field for wound healing.

Graphene and graphene oxide (GO) with excellent conductivity, unique physicochemical structure, and biocompatibility have risen to the forefront of the attention for their industrial, chemical, and biomedical applications [23]. Reduced GO is preferred to GO owing to its better conductivity and mechanical properties, which make it a promising reinforcing nanomaterial for tissue engineering [24]. Moreover, graphene tends to aggregate in aqueous media and the poor dispersion places a limit on its applications as a biomaterial [25, 26]. Herein, rGO was added to the polymeric network not only to provide electroconductivity but also to increase the mechanical properties, cell adhesion, proliferation and ultimately facilitate the wound healing process. Previous studies showed that incorporation of rGO into non-conductive polymeric material forms electroactive dressings for wound healing by providing a channel for electrical signal transmission [27, 28]. Furthermore, the immunomodulatory properties of GO provide it with significant advantages to overcome chronic diabetic ulcers [13, 29].

In the present study, polymeric nanofibers were prepared based on nanocrystal cellulose/reduced graphene oxide and polyvinyl alcohol (AD-CNCs/NH_2rGO/PVA). For this purpose, crystalline nanocellulose was prepared from cotton cellulose and oxidized in the presence of sodium periodate. Following the synthesis of reduced graphene oxide and its functionalization with amine, the crosslink between oxidized nanocrystalline cellulose and aminated reduced graphene oxide was created by

the Schiff-base reaction. The prepared nanocomposite was mixed with polyvinyl alcohol and different proportions of curcumin. Polymeric nanofibers were prepared by electrospinning. Synthesized compounds were characterized and the properties of nanofibers including mechanical properties, hydrophilicity, electroactivity, biocompatibility and degradability were also investigated.

2. Experimental

2.1. Materials and Methods

Cellulose nanocrystals (CNCs) were extracted from cotton and prepared by sulfuric acid hydrolysis. Sodium periodate ($NaIO_4$), and ethylene glycol were purchased from Sigma–Aldrich and used as received. Polyvinyl alcohol (Mw≈72000), N,N′-dicyclohexylcarbodiimide (DCC), 4-dimethylaminopyridine (DMAP) and *p*-anthranilic acid were purchased from Sigma-Aldrich and used without any purification. All other reagents were purchased from Merck and Sigma-Aldrich and purified according to the standard methods.

2.2. Preparation of CNC and AD-CNC

For the preparation of cellulose nanocrystals, first clean cotton (15 gr) was bleached using 500 mL of sodium hypochlorite at a temperature of 60°C for 4 hours. Then the obtained bleached cotton was washed several times with deionized water and dried for 3 days. The dried white cotton was hydrolyzed using 100 mL of sulfuric acid at 50°C for 4 hours.

After cooling the solution using an ice bath and washing it with distilled water several times, in order to adjust the pH of the obtained product to pH=7.8, sodium hydroxide solution and hydrochloric acid were used. For homogenization, it was sonicated with a bath-type sonicator for 15 min, and dried.

In order to prepare oxidized cellulose nanocrystals (AD-CNC), sodium periodate (0.24 gr, 1.13 mmol) was dissolved (1%w/v) in 40 mL aqueous suspension of cellulose nanocrystals and the reaction mixture was allowed to stir in a dark room for about 2 hours. Then, ethylene glycol (0.12 mL) was quickly added to the suspension to stop the oxidation reaction. Ultimately, the resultant suspension was dialyzed and dried [30,31].

2.3. Determination of aldehyde content

The grade of oxidation was determined by calculation of the aldehyde content. For this purpose, through the Schiff-base reaction, the oxidized cellulose nanocrystal was converted into oxide by hydroxylamine hydrochloride. In sodium hydroxide solution with pH=5, 20 ml of 0.72 M hydroxylamine hydrochloride was added to the oxidized cellulose nanocrystal solution and stirred for 24 hours at 40°C. The consumption amount of sodium hydroxide (V_c) was recorded and the nanocrystalline cellulose solution without oxidation was used as a control (V_b). The amount of aldehyde in the oxidized solution was calculated by the eq. 1. If the sodium hydroxide concentration is 0.5 M, m is the dry weight of oxidized cellulose nanocrystals, and M is the molecular mass of repeating units in oxidized cellulose nanocrystals [31,32].

$$\text{Aldehyde}(\%) = \frac{(V_c - V_b) \times M_{NaOH}}{\left(m/M_w\right)} \times 100 \quad (1)$$

2.4. Amination of graphene oxide (NH_2rGO)

The rGO was synthesized according to previous works [24, 33]. The NH_2rGO was prepared using the esterification method. Briefly, a 100-mL two-necked flask was charged with rGO(1 gr) and 4 mL of dimethylformamide (DMF). In order for homogenization, the suspension was sonicated with a bath-type sonicator for 10 min, and then dry 30 mL of tetrahydrofuran (THF) and anthranilic acid(27 mmol) were added. Next, 4-dimethylaminopyridine(30 mmol) and N, N′-dicyclohexylcarbodiimide(30 mmol) were introduced to the solution and the reaction mixture was de-aerated by bubbling highly pure argon for 10 min and stirred for 48 hours at ambient temperature. Succeeding the completion of the reaction, the precipitates were filtered and THF was removed and ultimately the product was dried at 60°C[31].

2.5. Electrospun nanofibers preparation

In order to prepare nanofibers, PVA, NH_2rGO and AD-CNCs in a ratio of 1:1:1 with different concentrations of curcumin (0.04 % and 0.08 % ratio for all compositions) were mixed in methanol solvent. Then electrospinning was performed at a feeding rate of 0.5 mL/hour with a voltage of 20 kV and a distance of 15 cm from the collector. The produced scaffold was collected on a rotating drum, dried in a vacuum oven and kept in a desiccator.

2.6. Biocompatibility test

An MTT assay was used to determine the cy-

totoxicity of prepared electrospun nanofibers. Primary Dermal Fibroblast; Normal, Human, Adult (HDFa) (ATCC PCS-201-012) were employed in the cytotoxicity tests. Cells were grown in Dulbecco's modified Eagle's medium (DMEM; Sigma-Aldrich, USA) containing 10% (v/v) fetal bovine serum (FBS) and antibiotics (100 mg/ml penicillin-streptomycin). Cells were seeded in 96-well plates with a density of 5×10^4 cells/ml and allowed to adhere overnight, and then treated with nanofibers (5×5 mm^2). After an incubation period of 1, 3 and 5 days, 50 mL of 3-[4,5-dimethylthiazol-2-yl]-2,5 diphenyl tetrazolium bromide (MTT) reagent (2 mg/mL in phosphate-buffered saline, PBS, pH 7.4, Invitrogen, CA, USA) was added to each well, followed by incubation at 37°C for 4 hours. The formazan crystals were dissolved in dimethyl sulfoxide and the UV absorbance was measured at 570 nm using an ELx 800 plate reader (Biotek, San Francisco, CA, USA) [31,34].

2.7. Characterization

The morphology of the prepared scaffolds was determined using field emission scanning electron microscope (FESEM) type 1430 VP (LEO Electron Microscopy Ltd, Cambridge, UK). Fourier transform infrared (FT-IR) spectra of the samples were evaluated at room temperature using a Shimadzu 8101 M FT-IR (Shimadzu, Kyoto, Japan) with a frequency range of 400-4000 cm^{-1} and equipped with an attenuated total reflection center. The thermal properties of the samples were evaluated using a thermogravimetric analyzer (TGA-PL STA 1640 equipment (Polymer Laboratories, Shropshire, UK). Thermogravimetric analyses (TGA) were conducted under a nitrogen atmosphere in a temperature ranging from 25°C to 700°C with a heating rate of 10°C/min^{-1}. Electrochemical data acquisition was performed using Auto-Lab PGSTAT302N (Metrohm, Switzerland). Electrochemical cell contained three electrodes (working, counter, and reference). Ultimate tensile strength and strain to failure were determined using a Zwick tensile tester (Z 010, Zwick/Roell, Ulm, Germany). The wettability of the electrospun nanofibers was evaluated by measuring the water droplet contact angle with an OCA 20 Plus goniometer system (DataPhysics Instruments GmbH, Filderstadt, Germany).

3. Results and discussion

Electrospinning is the most common way to manufacture nanofibers made of one polymer type, mixed polymers or polymers reinforced with different nanofillers. Addition of nanofiller reinforcements augments the properties of the fabricated electrospun nanofibers, including antibacterial and biological activity, porosity, and electrical and mechanical properties. Studies have introduced nanofillers such as metals and metal oxides (silver nanoparticles and titanium dioxide) and carbon-based materials (graphene nanosheets, graphene oxide and carbon nanotubes) to the fibrous matrix. Among these nanofillers, graphene, a single-layer two-dimensional (2D) crystalline, has been proven as a practical biocompatible material in several biomedical applications such as the development of scaffolds, drug delivery, imaging, and biosensors [23]. Incorporation of graphene nanosheets into nanofibers leads to the formation of highly oriented structures and networks inside polymer matrices modifying the electrical, mechanical, and thermal properties of the resulting composite [35, 36].

In this study, polymeric nanofibers were prepared based on nanocrystal cellulose/reduced graphene oxide and polyvinyl alcohol. The prepared nanocomposite was mixed with different proportions of curcumin and the polymeric nanofibers were prepared by electrospinning.

3.1. Characterization of nanofibers

3.1.1. Morphological study of produced nanofibers

Figure 1 presents SEM images of AD-CNCs/NH_2rGO/PVA nanofibrous composite without curcumin, and with 0.04% and 0.08% curcumin content. The polymeric structure of AD-CNCs/NH_2rGO/PVA possesses numerous pores. As can be seen, the morphology of the composite without curcumin has changed with presence of curcumin. With the increase of curcumin content, the diameter of the nanofibers increased from 40-100 nm for composite without curcumin, 700-750 nm for composite with 0.04% curcumin content to about 850-900 nm for composite with 0.08% curcumin content and the nanofibers presented a uniform morphology, while in the samples without curcumin, the nanofibers did not have a uniform diameter and morphology. Previous studies demonstrated similar alterations in fiber's morphology following the addition of curcumin [37, 38]. The distributed curcumin not only acts as an anti-oxidant but also plays a crucial role in reinforcing the fibrous matrix, contributing to enhanced mechanical properties and bioactivity [38].

3.1.2. FTIR analysis

Figure 2 demonstrates the FTIR spectra of AD-CNCs/NH_2rGO/PVA nanofibrous composite with and without curcumin content. The FTIR spectrum of rGO exhibits characteristic absorption bands due to stretching vibrations of aromatic C–H (3000–3100 cm^{-1}), the OH stretching vibration at 3475 cm^{-1}, and the C=C stretching vibration of the benzenoid units at 1550 cm^{-1}, and the C-O stretching vibration at 1176 cm^{-1}. A broad stretching vibration at 3419 cm^{-1} is detected in the FTIR spectrum of CNCs can be assigned to OH groups, and the C-O stretching vibration at 1114 cm^{-1}. The spectrum of PVA shows the OH groups stretching vibrations at 3400 cm^{-1}, and the absorption bands at 2800-2950 cm^{-1} due to stretching vibrations of aliphatic C–H. In the spectrum of AD-CNCs/NH_2rGO/PVA nanofibrous composite without curcumin, the absorption bands observed at 3400-3450 cm^{-1}, 2800-2950 cm^{-1} and 1610 cm^{-1} are due to the O-H groups of polyvinyl alcohol, aliphatic C-H and the imine group resulting from the Schiff-base crosslink respectively. The band at 1600-1400 cm^{-1} corresponds to the C=C bonds of curcumin.

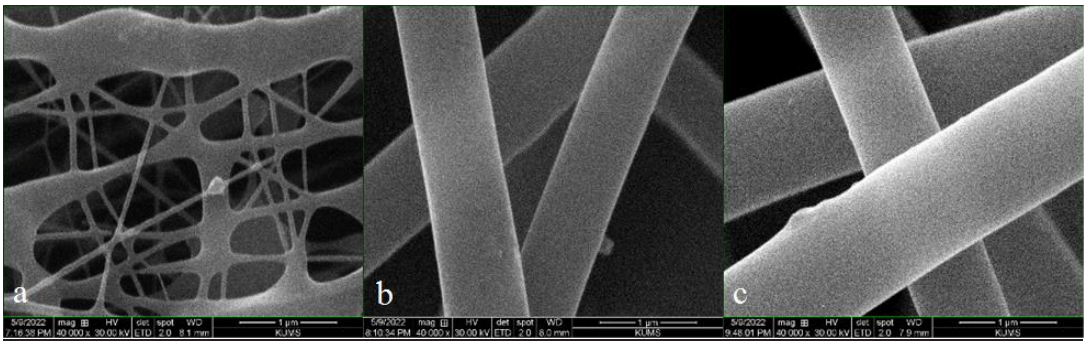

Fig. 1- FE-SEM images of AD-CNCs/NH_2rGO/PVA nanofibrous matrix without curcumin (a), with 0.04% (b) and 0.08% (c) curcumin.

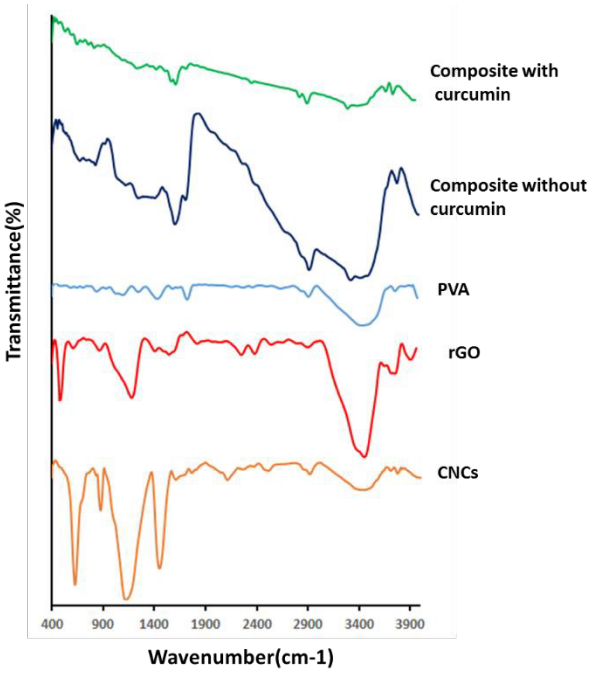

Fig. 2- FT-IR spectra of CNCs, rGO, PVA, Composite with and without curcumin.

3.1.3. XRD

XRD patterns of rGO are shown in Figure 3 (red). For rGO, the amorphous surface corresponding to the reduced graphene oxide at 2θ=26 can be seen. XRD patterns of CNCs with typical features are shown in Figure 3 (blue). The peaks related to the crystalline surfaces of cellulose nanocrystals are seen at 2θ=23.3, 29.14, 32.1, 34.1, and 47.9. As can be seen in XRD patterns of composite without curcumin (navy blue), the created crystalline surfaces are different from rGO and CNCs, because the crosslink between the two compounds changes crystalline surfaces creating new crystalline regions. Moreover, the polyvinyl alcohol has semi-crystalline surfaces around degrees 19 and 39, related to intermolecular and intramolecular hydrogen bonds. The XRD patterns of composite with 0.04% curcumin demonstrate the crystal levels related to curcumin up to the 2θ=30, such as 7.96, 8.90, 12.26, 14.54, and 17.24. The crystalline surfaces related to the combination of PVA/AD-CNCs/NH_2rGO are also seen in the sample. It seems that compared to the sample without curcumin, the peaks have overlapped, but the intensity of the peaks has increased. Furthermore ,crystallit sizes and lattice parameters for samples are shown in Table 1. As can be seen in Table 1, the lattice strain in the composite and also with the addition of curcumin increases. Also, the crystallite size in the composite with curcumin has decreased compared to other samples. In addition, in XRD spectra, the degree of crystallinity increases with the sharpening of the peaks.

3.1.4. Thermal stability

The thermogravimetric analysis of CNCs, PVA/AD-CNCs/NH_2rGO and PVA/AD-CNCs/NH_2r-

Table 1- Crystallit sizes and lattice parameters for samples

Sample	d-spacing(°A)	FWHM(°)	Crystallit size(°A) (Sherrer method)	Lattice Strain(%) (Sherrer method)
composite with curcumin	5.1014	0.2362	341	0.674
CNCs	2.6467	0.1181	704	0.169
rGO	3.4654	0.2362	345	0.451
Composite without curcumin	11,3615	0.098	813	0.629

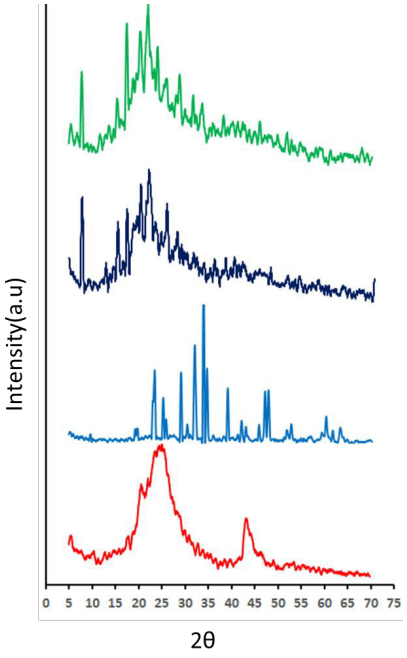

Fig. 3- XRD spectra of rGO (red), CNCs (blue), Composite without curcumin (Navy blue), and composite with curcumin (green).

GO scaffold containing curcumin were carried out to determine the weight changes in relation to temperature increase. According to the TGA curves (Fig. 4), from the ambient temperature (24˚C) to 100˚C, there is a slight weight loss in the samples due to the evaporation of adsorbed water. By increasing the temperature up to 349.09 ˚C, 334.4 ˚C and 384.9 ˚C there is a large loss of mass in CNCs, PVA/AD-CNCs/NH_2rGO and PVA/AD-CNCs/NH_2rGO/curcumin samples respectively, destroying 65%, 46.7% and 41.1% of the compositions. Cellulose has a high ability to absorb moisture; therefore, this result can be due to dehydration and loss of remaining moisture. Degradation temperature of cellulose has been reported to be 300-450˚C, depending on various additives and bondings [39]. As can be observed addition of PVA and curcumin to the fibrous matrix increased the decomposition temperature. At 700˚C, only 19.8% of CNCs, 9.1% of the composite without curcumin and 12.1% of the composite with curcumin remained.

3.1.5. Electroactivity

Cyclic voltammetry is a tool for measuring the electrical activity of compounds, which can be an advantage in tissue engineering since electrical signals are useful for proliferation, adhesion and differentiation of different types of cells. CV voltammograms were recorded using 1 M H_2SO_4 with a potential range of -0.2 to +1.2 V vs. Ag/AgCl at a scan rate of 10-50 mV s^{-1} [35].

As can be seen in Figure 5, compounds containing rGO showed a pair of redox peaks. The displacement of the anode peaks is towards higher potentials with increasing scan rates. Therefore, the oxidation/reduction of polymer films is chemically reversible.

3.1.6. Water contact angle

Images of water drop on composite without curcumin, composite with 0.04% curcumin and composite with 0.08% curcumin are shown in Figure 6. The bioactivity of dressing scaffolds as the

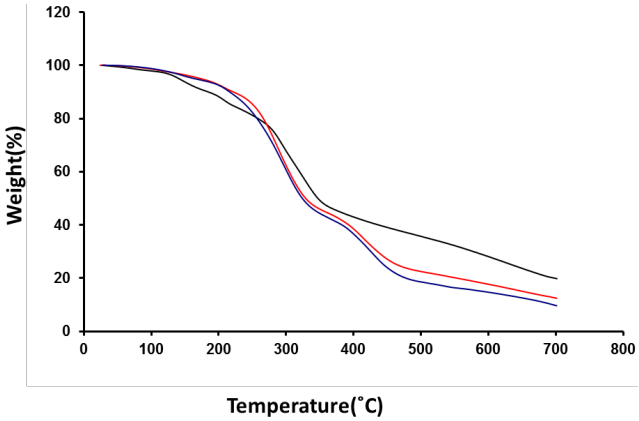

Fig. 4- PVA/AD-CNCs/NH2rGO (blue), PVA/AD-CNCs/NH2rGO /Curcumin (red), and CNCs (black).

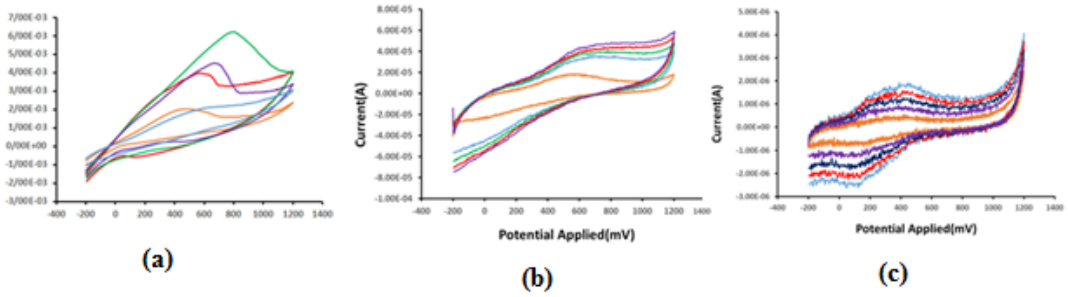

Fig. 5- CVs of rGo (a), NH2rGO-CNCs (b), and scaffold without curcumin (c) using 1 M H2SO4 with a potential range of -0.2 to +1.2 V at a scan rates of 10-50 mV s^{-1}.

fibroblast adhesion, and proliferation on the nanofibrous matrix depends on its hydrophilic nature. The contact angle of water to nanofibers shows that by increasing the amount of curcumin, the composition becomes more hydrophobic. The PVA/AD-CNCs/NH_2rGO scaffold is highly hydrophilic with a WCA of 15.80°, however, the scaffold with 0.04% and 0.08% curcumin exhibit a WCA of 101.91° and 112.48° respectively. Previous studies also corroborated that the addition of curcumin to a nanofibrous scaffold decreases its hydrophilicity [37].

3.2. Biodegradability

The degradation of the electrospun nanofibrous scaffold depends on various factors, including their hydrophobic nature, geometrical and morphological properties and environmental factors such as pH and temperature. In this work, SEM was used to indicate the degradability of nanofibers. The image of the degradability of nanofibers after 10 days of immersion in PBS solution at 37°C is shown in Figure 7.

3.3. Mechanical properties

The mechanical properties of engineered scaffolds are a crucial factor for tissue engineering and wound healing since they affect cell-scaffold interactions, cell adhesion, growth, and signaling procedures. For instance, the elasticity of scaffolds affects cellular activity such as cell distribution and differentiation. The wound dressings have to be strong enough to be applied to the wound site and readily removed without causing any damage to the newly formed tissues. Furthermore, the stiffness controls the cell-scaffold interactions. Cell adhesion and stretching along the matrix necessitate sufficient stiffness to resist the deformations by cell tractions [40].

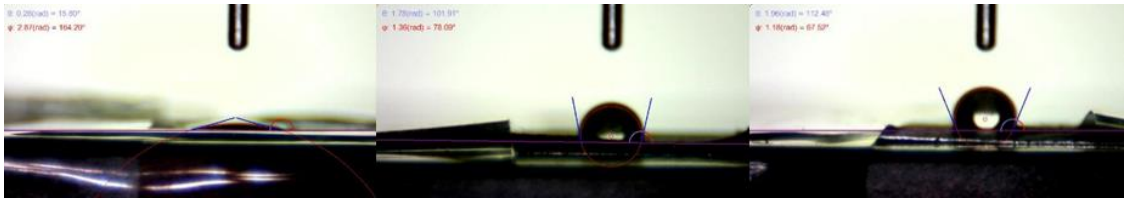

Fig. 6- Contact angle images of scaffold without curcumin (a), scaffold with curcumin (0.04%) (b) and scaffold with curcumin (0.08%) (c).

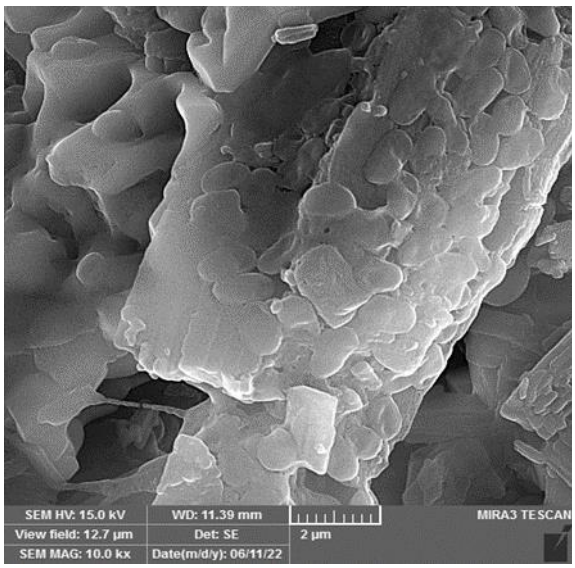

Fig. 7- FE-SEM image of nanofibers in-vitro degradability after 10 days of immersion in PBS at 37°C.

Mechanical parameters of the synthesized nanofibers are presented in Table 2. The obtained results show that with the increase of curcumin content, the amount of Young's modulus of nanofibers has increased, as the scaffold with 0.08% curcumin is stiffer than other groups. The tensile strength of the scaffold decreased with addition of 0.04% curcumin and the elongation at break was found to be higher with the PVA/AD-CNCs/NH_2rGO scaffold without curcumin. This correlates with studies report-

Table 2- Mechanical properties of scaffolds

Sample	Young's Modulus (MPa)	Tensile Strength (MPa)	Elongation at break (%)
Scaffold without curcumin	32.94±1.45	15.07±0.8	66.58±4.3
Scaffold with curcumin (0.04%)	90.99±4.6	5.95±0.2	32.40±1.7
Scaffold with curcumin (0.08%)	167.79±9.20	6.48±0.16	43.19±2.05

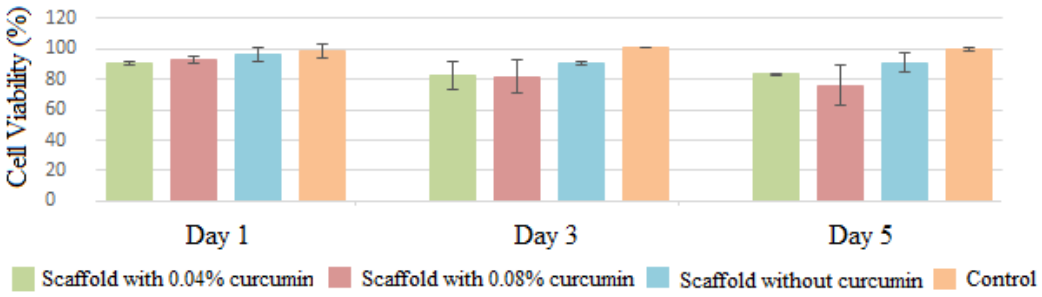

Fig. 8- In vitro cytotoxicity effects of fabricated scaffolds on HDFa cells.

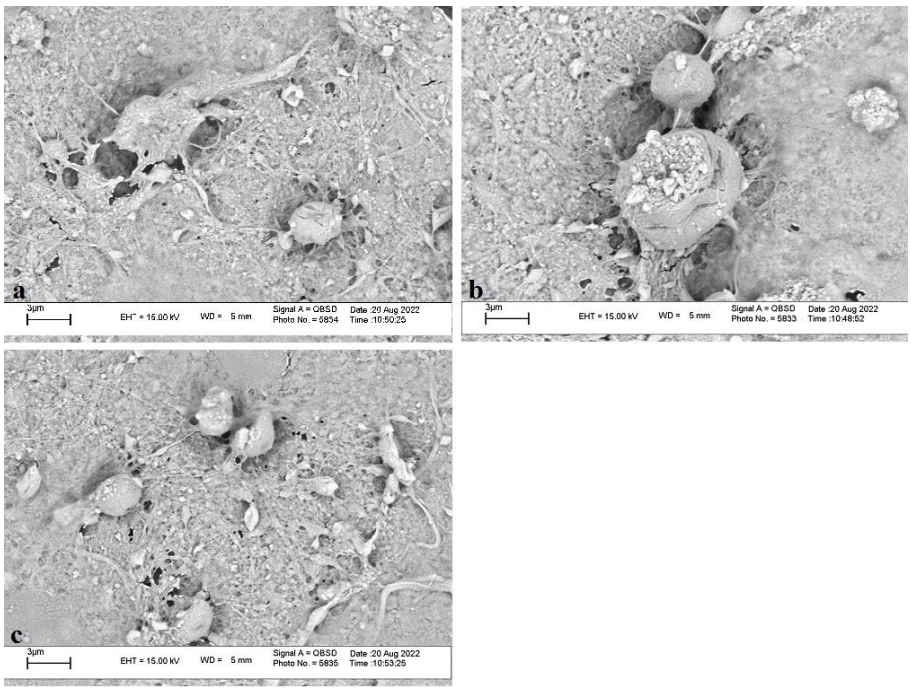

Fig. 9- Morphology of fibroblasts on scaffold with 0.04% curcumin (a), scaffold with 0.08% curcumin (b) and scaffold without curcumin(c).

ing that the mechanical strength of fibrous scaffolds is controllable by the ratio of their additives. The mechanical properties of the scaffolds are adjusted according to the type of tissue. Several studies suggest that nanofibrous scaffolds with tensile strength ranging from 0.7 to 18 MPa are suitable for dermal applications [40, 41].

3.4. Biocompatibility

Biocompatibility of biomaterials is an essential requirement for their application in wound healing due to its direct effect on cell attachment, proliferation, migration, differentiation and ultimately new tissue formation. The cytotoxicity of electrospun nanofibers was investigated by MTT assay at an initial seeding density of 5 $\times 10^4$ cells/mL using HDFa cells. As shown in Figure 8 compared to the control sample, the fabricated wound healing scaffolds were conductive to HDFa cells proliferation. No significant difference is detectable in cell viability between scaffolds at days 1 and 3. The slight difference might be due to the reduced hydrophilicity of fibrous scaffold following the addition of curcumin, which has a noticeable effect in cell adherence and proliferation.

Structural properties of fabricated biomaterials regulate the cell and scaffold interactions, cellular signaling, nutrients transport and biological molecular activity for cell proliferation and deposition of ECM, initiating a cascade of biological processes leading to tissue repair. It has been shown that cells prefer to attach and penetrate the fibrous scaffolds with thicker fibers. Moreover, the surface porosity and wettability affect the cell attachment and spreading capabilities [40]. The SEM images (Fig. 9) of the cultured fibroblast cells on scaffolds showed that all fabricated nanofibrous scaffolds support cell morphology, attachment and spreading indicating that the nanoporous topology of the fiber scaffolds affects the fibroblast's activity. Fibroblast cells grown on the scaffolds containing curcumin showed irregular stretched morphology with an increased number of cells. Although the hydrophilicity of the curcumin-containing scaffolds was lower than the ones without curcumin, the increased fiber diameter, nanoporous structure and presence of curcumin resulted in high cell impregnation in the scaffolds. The results demonstrated that PVA/AD-CNCs/NH_2rGO nanofibrous scaffolds with and without curcumin content can support the high proliferation of fibroblasts with cell growth and spreading as a wound dressing material. The scaffolds containing curcumin presented an acceptable performance in terms of cell spreading and cell density suggesting them as a potential candidate for wound dressing.

4. Conclusion

Electroactive dressings containing conductive biomaterials, which have conductivity comparable to the skin, can reportedly accelerate wound regeneration and repair [8]. Therefore, in the present work, electroactive wound dressings were prepared based on AD-CNCs/NH_2rGO/PVA with different ratios of curcumin as an anti-inflammatory agent. The morphology, electroactivity and hydrophilicity of nanofibers were investigated and the results showed that with the increase in curcumin content, the hydrophobicity of the composition and the diameter of the nanofibers increases, while the uniformity and mechanical properties are optimized. Overall, PVA/AD-CNCs/NH_2rGO/curcumin nanofibrous scaffolds are a potential candidate for wound dressing since the scaffolds presented a satisfactory performance in cell attachment, proliferation and spreading, requirements for wound healing purposes.

Conflict of interest

Authors declare that they have no conflict of interest.

Acknowledgments

Financial support from Payame Noor University is gratefully acknowledged.

References

1. Raziyeva K, Kim Y, Zharkinbekov Z, Kassymbek K, Jimi S, Saparov A. Immunology of acute and chronic wound healing. Biomolecules. 2021;11(5):700.
2. Nussbaum SR, Carter MJ, Fife CE, DaVanzo J, Haught R, Nusgart M, et al. An economic evaluation of the impact, cost, and medicare policy implications of chronic nonhealing wounds. Value in Health. 2018;21(1):27-32.
3. Yousefi K, Hamedeyazdan S, Hodaei D, Lotfipour F, Baradaran B, Orangi M, et al. An in vitro ethnopharmacological study on Prangos ferulacea: a wound healing agent. BioImpacts: BI. 2017;7(2):75.
4. Mansoub NH, Gürdal M, Karadadaş E, Kabadayi H, Vatansever S, Ercan G. The role of PRP and adipose tissue-derived keratinocytes on burn wound healing in diabetic rats. BioImpacts: BI. 2018;8(1):5.
5. Guo B, Dong R, Liang Y, Li M. Haemostatic materials for wound healing applications. Nature Reviews Chemistry. 2021;5(11):773-91.
6. Karimian R, Mehrabani MG, Mehramuz B, Ganbarov K, Ejlali

L, Tanomand A, et al. Poly (ε-Caprolactone)/cellulose nanofiber blend nanocomposites containing ZrO2 nanoparticles: A new biocompatible wound dressing bandage with antimicrobial activity. Advanced Pharmaceutical Bulletin. 2020;10(4):577.
7. Umar NM, Parumasivam T, Toh S-M. An overview of cutaneous wounds and the beneficial roles of medicinal plants in promoting wound healing. Pharmaceutical Sciences. 2021;27(4):489-502.
8. Korupalli C, Li H, Nguyen N, Mi FL, Chang Y, Lin YJ, et al. Conductive materials for healing wounds: their incorporation in electroactive wound dressings, characterization, and perspectives. Advanced healthcare materials. 2021;10(6):2001384.
9. Ning C, Zhou Z, Tan G, Zhu Y, Mao C. Electroactive polymers for tissue regeneration: Developments and perspectives. Progress in polymer science. 2018;81:144-62.
10. Li S, Wang L, Zheng W, Yang G, Jiang X. Rapid fabrication of self-healing, conductive, and injectable gel as dressings for healing wounds in stretchable parts of the body. Advanced Functional Materials. 2020;30(31):2002370.
11. Zhao X, Guo B, Wu H, Liang Y, Ma PX. Injectable antibacterial conductive nanocomposite cryogels with rapid shape recovery for noncompressible hemorrhage and wound healing. Nature communications. 2018;9(1):2784.
12. Nguyen N, Lin Z-H, Barman SR, Korupalli C, Cheng J-Y, Song N-X, et al. Engineering an integrated electroactive dressing to accelerate wound healing and monitor noninvasively progress of healing. Nano Energy. 2022;99:107393.
13. Ou X, Guan L, Guo W, Zhang X, Wu S, Guo D, et al. Graphene oxide-based injectable conductive hydrogel dressing with immunomodulatory for chronic infected diabetic wounds. Materials & Design. 2022;224:111284.
14. Wu C, Shen L, Lu Y, Hu C, Liang Z, Long L, et al. Intrinsic antibacterial and conductive hydrogels based on the distinct bactericidal effect of polyaniline for infected chronic wound healing. ACS Applied Materials & Interfaces. 2021;13(44):52308-20.
15. Chowdhury NA, Al-Jumaily AM. Regenerated cellulose/polypyrrole/silver nanoparticles/ionic liquid composite films for potential wound healing applications. Wound Medicine. 2016;14:16-8.
16. Xiong F, Wei S, Sheng H, Wu S, Liu Z, Cui W, et al. Three-layer core-shell structure of polypyrrole/polydopamine/poly (l-lactide) nanofibers for wound healing application. International Journal of Biological Macromolecules. 2022;222:1948-62.
17. Sarvari R, Massoumi B, Zareh A, Beygi-Khosrowshahi Y, Agbolaghi S. Porous conductive and biocompatible scaffolds on the basis of polycaprolactone and polythiophene for scaffolding. Polymer Bulletin. 2020;77:1829-46.
18. Hakkarainen T, Koivuniemi R, Kosonen M, Escobedo-Lucea C, Sanz-Garcia A, Vuola J, et al. Nanofibrillar cellulose wound dressing in skin graft donor site treatment. Journal of Controlled Release. 2016;244:292-301.
19. Zineh BR, Roshangar L. An experimental study on the mechanical and biological properties of bio-printed alginate/halloysite nanotube/methylcellulose/Russian olive-based scaffolds. Advanced Pharmaceutical Bulletin. 2018;8(4):643.
20. Czaja W, Krystynowicz A, Kawecki M, Wysota K, Sakiel S, Wróblewski P, et al. Biomedical applications of microbial cellulose in burn wound recovery. Cellulose: Molecular and Structural Biology: Selected Articles on the Synthesis, Structure, and Applications of Cellulose. 2007:307-21.
21. Sarvari R, Keyhanvar P, Agbolaghi S, Roshangar L, Bahremani E, Keyhanvar N, et al. A comprehensive review on methods for promotion of mechanical features and biodegradation rate in amniotic membrane scaffolds. Journal of Materials Science: Materials in Medicine. 2022;33(3):32.
22. Baghaie S, Khorasani MT, Zarrabi A, Moshtaghian J. Wound healing properties of PVA/starch/chitosan hydrogel membranes with nano Zinc oxide as antibacterial wound dressing material. Journal of Biomaterials Science, Polymer Edition. 2017;28(18):2220-41.
23. Chung C, Kim Y-K, Shin D, Ryoo S-R, Hong BH, Min D-H. Biomedical applications of graphene and graphene oxide. Accounts of chemical research. 2013;46(10):2211-24.
24. Sarvari R, Sattari S, Massoumi B, Agbolaghi S, Beygi-Khosrowshahi Y, Kahaie-Khosrowshahi A. Composite electrospun nanofibers of reduced graphene oxide grafted with poly (3-dodecylthiophene) and poly (3-thiophene ethanol) and blended with polycaprolactone. Journal of Biomaterials science, Polymer edition. 2017;28(15):1740-61.
25. Aycan D, Selmi B, Kelel E, Yildirim T, Alemdar N. Conductive polymeric film loaded with ibuprofen as a wound dressing material. European Polymer Journal. 2019;121:109308.
26. Wen Y, Wen W, Zhang X, Wang S. Highly sensitive amperometric biosensor based on electrochemically-reduced graphene oxide-chitosan/hemoglobin nanocomposite for nitromethane determination. Biosensors and Bioelectronics. 2016;79:894-900.
27. Agbolaghi S, Abbaspoor S, Massoumi B, Sarvari R, Sattari S, Aghapour S, et al. Conversion of Face-On Orientation to Edge-On/Flat-On in Induced-Crystallization of Poly (3-hexylthiophene) via Functionalization/Grafting of Reduced Graphene Oxide with Thiophene Adducts. Macromolecular Chemistry and Physics. 2018;219(4):1700484.
28. Khodaee Z, Mazinani S, Sharif F. Reduced graphene oxide-modified polyvinyl alcohol hydrogel with potential application as skin wound dressings. Journal of Polymer Research. 2023;30(1):5.
29. Orsu P, Haider HY, Koyyada A. Bioengineering for curcumin loaded carboxymethyl guargum/reduced graphene oxide nanocomposites for chronic wound healing applications. International Journal of Pharmaceutics. 2021;606:120928.
30. Pandi N, Sonawane SH, Kishore KA. Synthesis of cellulose nanocrystals (CNCs) from cotton using ultrasound-assisted acid hydrolysis. Ultrasonics sonochemistry. 2021;70:105353.
31. Massoumi B, Sarvari R, Fakhri E. Conductive electrospun nanofiber based on silk fibroin/cellulose nanocrystals/reduced graphene oxide as a wound healing material. International Journal of Polymeric Materials and Polymeric Biomaterials. 2023 Oct 17:1-0.
32. Nezhad-Mokhtari P, Akrami-Hasan-Kohal M, Ghorbani M. An injectable chitosan-based hydrogel scaffold containing gold nanoparticles for tissue engineering applications. International journal of biological macromolecules. 2020;154:198-205.
33. Zeighami M, Agbolaghi S, Hamdast A, Sarvari R. Graphenic nanosheets sandwiched between crystalline cakes of poly (3-hexylthiophene) via simultaneous grafting/crystallization and their applications in active photovoltaic layers. Journal of Materials Science: Materials in Electronics. 2019;30:7018-30.
34. Sarvari R, Agbolaghi S, Beygi-Khosrowshahi Y, Massoumi B. Towards skin tissue engineering using poly (2-hydroxy ethyl methacrylate)-co-poly (N-isopropylacrylamide)-co-poly (ε-caprolactone) hydrophilic terpolymers. International Journal of Polymeric Materials and Polymeric Biomaterials. 2019;68(12):691-700.
35. Ali IH, Ouf A, Elshishiny F, Taskin MB, Song J, Dong M, et al. Antimicrobial and wound-healing activities of graphene-reinforced electrospun chitosan/gelatin nanofibrous nanocomposite scaffolds. ACS omega. 2022;7(2):1838-50.
36. Wang C, Li Y, Ding G, Xie X, Jiang M. Preparation and characterization of graphene oxide/poly (vinyl alcohol) composite nanofibers via electrospinning. Journal of Applied Polymer Sci-

ence. 2013;127(4):3026-32.
37. Pandey VK, Ajmal G, Upadhyay SN, Mishra PK. Nano-fibrous scaffold with curcumin for anti-scar wound healing. International Journal of Pharmaceutics. 2020;589:119858.
38. Suteris NN, Yasin A, Misnon II, Roslan R, Zulkifli FH, Rahim MHA, et al. Curcumin loaded waste biomass resourced cellulosic nanofiber cloth as a potential scaffold for regenerative medicine: An in-vitro assessment. International Journal of Biological Macromolecules. 2022;198:147-56.
39. D'Acierno F, Hamad WY, Michal CA, MacLachlan MJ. Thermal Degradation of Cellulose Filaments and Nanocrystals. Biomacromolecules. 2020;21(8):3374-86.
40. Lanno G-M, Ramos C, Preem L, Putrins M, Laidmae I, Tenson T, et al. Antibacterial porous electrospun fibers as skin scaffolds for wound healing applications. ACS omega. 2020;5(46):30011-22.
41. Mistry P, Chhabra R, Muke S, Narvekar A, Sathaye S, Jain R, et al. Fabrication and characterization of starch-TPU based nanofibers for wound healing applications. Materials Science and Engineering: C. 2021;119:111316.